Carbohydrate Polymers 181 (2018) 247–255

Contents lists available at ScienceDirect

Carbohydrate Polymers

journal homepage: www.elsevier.com/locate/carbpol

Research paper

Post-sulfonation of cellulose nanofibrils with a one-step reaction to improve dispersibility

Jeffrey Luo[a,b], Nikolay Semenikhin[a,b], Huibin Chang[a,b], Robert J. Moon[a,b,c], Satish Kumar[a,b,*]

[a] School of Materials Science and Engineering, Georgia Institute of Technology, Atlanta, GA 30332, USA
[b] Renewable Bioproducts Institute, Georgia Institute of Technology, Atlanta, GA, USA
[c] The Forest Products Laboratory, US Forest Service, Madison, WI 53726, USA

ARTICLE INFO

Keywords:
Cellulose sulfate
Cellulose nanofibrils
Cellulose

ABSTRACT

Cellulose nanofibrils (CNF) were sulfonated and the dispersion quality was compared to unfunctionalized and 2,2,6,6-tetramethylpiperdine-1-oxyl radical (TEMPO) post-oxidation treatment of existing CNF (mechanically fibrillated pulp). A post-sulfonation treatment on existing CNF in chlorosulfonic acid and dimethylformamide (DMF) resulted in sulfonated CNF that retained a fibril-like morphology. There was a small decrease in the cellulose crystallinity index for the sulfonated CNF, but this was much lower than the reported regioselective oxidative bisulfite pretreatment method used to make sulfonated CNF. The current approach was extremely quick, and 5 min of reaction time was sufficient to result in significant improvements in dispersibility compared to unfunctionalized CNF. The sulfonated CNF and TEMPO oxidized CNF had better dispersibility compared to the unfunctionalized CNF when dispersed in DMF and water, and in many cases the sulfonated CNF had better dispersibility than the TEMPO CNF. It was found that when CNF was dispersed in DMF the TEMPO CNF formed carboxyl dimethylammonium groups, while the sulfonated CNF formed formate groups.

1. Introduction

Cellulose nanomaterials (CNM) are a new class of cellulose base particles that can be extracted from plants and trees. CNM are distinct from molecular cellulose and wood pulp, having a new combination of properties and functionalities (e.g. high surface area, biodegradability, biorenewability, low toxicity, and high mechanical properties) that are being utilized in the development of applications that were once thought impossible for cellulosic materials (Habibi, Lucia, & Rojas, 2010; Lin & Dufresne, 2014a; Moon, Schueneman, & Simonsen, 2016; Nechyporchuk, Belgacem, & Bras, 2016; Siqueira, Bras, & Dufresne, 2010; Siró & Plackett, 2010). There are many different types of CNM, as a consequence from their extraction/production process, in which the differing morphology and surface chemistries can strongly influence how a particular CNM interacts with its environment (Habibi, 2014; Moon et al., 2016; Nechyporchuk et al., 2016). One type of CNM is cellulose nanofibrils (CNF), which are produced by mechanical shearing of the wood pulp fibers. CNF have a flexible fiber/fibril morphology, aspect ratios of ~10 to 100, length greater than 1 μm, with diameters ~20 to 100 nm, and a surface chemistry of terminating hydroxyl groups. Finer diameter fibrils (~4 to 10 nm) can be produced if pretreatments are used prior to mechanical refinement, the most common of which is a chemical treatment with 2,2,6,6-tetramethylpiperdine-1-oxyl radical (TEMPO) mediated oxidation, resulting in carboxylic acid surface groups. The resulting material is commonly referred to as TEMPO CNF (Saito, Kimura, Nishiyama, & Isogai, 2007).

One of the difficulties in working with CNM is how to effectively disperse these materials in a wide variety of solvents and polymers, which is necessary for them to reach their full potential (e.g. mechanical reinforcement capacity in polymer composites) (Chang et al., 2015; Chang, Luo, Gulgunje, & Kumar, 2017; Luo et al., 2017). Various chemical functionalizations have been explored in making CNM more compatible to a given environment to improve dispersibility (Espino-Pérez, Domenek, Belgacem, Sillard, & Bras, 2014; Habibi, 2014). For improving CNF dispersion, the most common is TEMPO oxidation, where the resulting carboxylic acid groups on the CNF surface gives increased surface charge (Isogai, 2013; Nechyporchuk et al., 2016). Typically, this surface modification is done as chemical pretreatment in the TEMPO CNF fabrication process. Studies focusing on post TEMPO oxidation of existing CNF (mechanically fibrillated pulp) are limited, however, there are studies on post TEMPO oxidation of cellulose nanocrystals (CNC) that have shown to improve dispersion in various

* Corresponding author at: School of Materials Science and Engineering, Georgia Institute of Technology, 801 Ferst Dr., Atlanta, Georgia 30332-0295, USA.
E-mail addresses: JLuo73@gatech.edu (J. Luo), NSemenikhin3@gatech.edu (N. Semenikhin), Hbchang@gatech.edu (H. Chang), Robertmoon@fs.fed.us (R.J. Moon), Satish.Kumar@gatech.edu (S. Kumar).

http://dx.doi.org/10.1016/j.carbpol.2017.10.077
Received 28 August 2017; Received in revised form 6 October 2017; Accepted 22 October 2017
Available online 23 October 2017
0144-8617/

solvents (Araki, Wada, & Kuga, 2001; Habibi, Chanzy, & Vignon, 2006).

Another approach, which has seen less attention, is sulfonation of CNF to produce sulfate half ester groups, to give sufficient surface charge for increased dispersibility (Habibi, 2014; Nechyporchuk et al., 2016). This dispersion mechanism is akin to that of cellulose nanocrystals (CNC) produced by sulfuric acid hydrolysis (Chang et al., 2016; Nagasawa, Tohira, Inoue, & Tanoura, 1971; Viet, Beck-Candanedo, & Gray, 2007). Incidentally, cellulose sulfate, which is cellulose that has been sulfonated, has been made with many different reaction schemes since the 1800s (Nagasawa et al., 1971), and has been considered for use as an anti-coagulant (Wang, Li, Zheng, Normakhamatov, & Guo, 2007), flocculant (Nourani, Baghdadi, Javan, & Bidhendi, 2016), and in other applications (Schweiger, 1979). Typically however, in these studies soluble cellulose (e.g. fibril structure is dissolved), or cellulose agglomerates (e.g. cellulose fibrils fuse together) are made (Schweiger, 1972; Svensson et al., 2005; Zhang, Peschel, Bäucker, Groth, & Fischer, 2011), and neither morphology is suitable for mechanical reinforcement due to the loss of the fibril structure leading to lower mechanical reinforcement capacity. Recent studies on sulfonating CNF with a regioselective oxidative bisulfite pretreatment have been successful, but this reaction scheme leads to the cleavage of the cellulose rings, and has been shown to reduce the crystallinity of the resulting CNF (Liimatainen, Visanko, Sirviö, Hormi, & Niinimäki, 2013). The decrease in crystallinity might have detrimental effects on the mechanical properties (Chen, Lickfield, & Yang, 2004; Wu, Moon, & Martini, 2014).

The TEMPO and regioselective oxidative bisulfite pretreatment results in cellulose in the form of a sodium salt derivative. This sodium salt form of the functionalization on cellulose does not allow hydrogen bonding to form. For cases where hydrogen bonding is desired (e.g. improve load transfer between CNFs for higher mechanical properties), extra time for completed protonation reactions is needed. In contrast, the sulfonation reaction discussed in this paper is a one-step reaction that results in the acid form of cellulose sulfate.

The goal of this study was to develop a sulfonation process on existing CNF that can functionalize CNF surface with sulfate half ester groups while retaining the CNF's fibril-like morphology. The effect of reaction time on CNF morphology, crystallinity index, chemical structure, CNF dispersion in water and in dimethylformamide (DMF), is reported and compared to unfunctionalized and post-TEMPO oxidized CNF. Lastly the effects of heating in either water or DMF was explored as many processes to form nanocomposites involves heating the materials in solvents.

2. Experimental

2.1. Material

Freeze dried CNF (Lot #U38) produced by mechanical treatment at the Process Development Center, University of Maine, were used in this study. Anhydrous DMF, TEMPO free radical (98%), sodium hypochlorite (NaClO) (14.5% available chlorine in water), sodium hydroxide (NaOH), and hydrochloric acid (HCl) (36 wt%) was obtained from Alfa Aesar. Chlorosulfonic acid (CSA), sodium chloride (NaCl) (99.5%), and DMF (distilled before use) was obtained from Sigma-Aldrich Corporation. Sodium bromide (NaBr) was obtained from Fisher Scientific. Potassium bromide (KBr) was obtained from Specac Ltd. Dialysis Tubing 14,000 MW cutoff was obtained from Ward's Science.

2.2. Functionalization of cellulose nanofibrils

Three different sulfonations were completed with varying moles of CSA to anhydroglucose units (AGU) ratios of 0.5:1, 1.5:1, and 2.5:1, these samples will be referred to as SCNF1, SCNF2, and SCNF3, respectively. For the sulfonation reaction, nitrogen was constantly flowed through the system to prevent water from the air to get into the system. Also all the glassware was dried in an oven at 110 °C overnight to remove all adsorbed water before use. In a three neck flask, 4 g of freeze dried CNF was added to 400 mL of DMF and left for 30 min to let the CNF absorb the DMF. This mixture was then homogenized with an IKA T18 basic Ultra-Turrax for 5 min (at a setting of 3.5) followed by another 15 min soak and 5 min of homogenization (at a setting of 3.5). Due to the small amount of CSA being used to increase accuracy a large batch of DMF and CSA was prepared, in which 35 mL of DMF was chilled in an ice bath for 10 min before 7 mL of CSA was slowly added into the DMF while undergoing stirring. The desired amount of this CSA/DMF solution was slowly added (~1 min) to the CNF/DMF mixture while undergoing stirring. For each different CSA to AGU ratio sulfonation experiment 1 batch was made and multiple samples were taken out after 5, 30, and 60 min after the CSA/DMF solution was added. For the naming scheme the samples will be referred to as SCNF1-5, SCNF1-30, and SCNF1-60 for the 0.5:1 CSA to AGU ratio samples that reacted for 5, 30, and 60 min, respectively, and with the SCNF2 and SCNF3 samples following the same naming scheme. The reaction was stopped after taking out the sample by adding 1 mL of methanol for every 5 mL of sample taken out. Samples were washed multiple times by centrifugation (15,000 × *g*) with deionized (DI) water until the pH of the supernatant was neutral (pH strips were used) followed by two additional washings. This process was also repeated with a 0:1 CSA to AGU ratio with a sample taken after 60 min of stirring to be used as the control sample and will be referred to as unfunctionalized CNF in the rest of the paper.

The post TEMPO oxidation on existing CNF was completed with a molar ratio of 2:1 NaClO:AGU. In a three neck flask, 4 g of freeze dried CNF was added to 400 mL of DI water and left for 30 min. This mixture was then homogenized with an IKA T18 basic Ultra-Turrax for 5 min followed by another 15 min soak and another 5 min of homogenization with the same settings mentioned above. Then 0.08 g of TEMPO free radical and 0.5 g NaBr was added to the suspension while undergoing stirring with a stir bar and was stirred for 1 h to make sure the chemicals were dissolved. The pH of the suspension was adjusted to 10.5 by adding 0.5 M NaOH aqueous solution. The pH was monitored with a pH meter UltraBASIC (Denver Instruments). Then 25.7 g of NaClO aqueous solution (14.5 wt%) was added drop wise, after this addition, the pH was monitored and adjusted to stay between 10 and 10.5 by adding 0.5 M NaOH aqueous solution. Once the pH stabilizes the reaction is finished (~2 h), and 23.5 g of NaCl was added to flocculate the CNF. The suspension was then centrifuged (15,000 × *g*) and washed with 1 M NaCl aqueous solution 4 times. The CNF was then protonated by stirring overnight in 1 L of 0.1 M HCl aqueous solution. Afterward the CNF was centrifuged and washed with DI water until the pH of the supernatant was neutral (pH strips were used), followed by two additional washings. CNF were then put in dialysis bags and dialyzed in a large container with DI water. The water was changed every 2 h for the first 3 exchanges followed by water exchanges two times a day for 3 days. After this process it was determined that the CNF was not fully protonated and still contained COO^- groups attributed to the COONa. Consequently, 0.7 g of this CNF was further protonated in 100 mL of 0.25 M HCl for 24 h. Then the same cleaning process used before was followed without the dialysis step. Only this fully protonated CNF will be used for characterization and discussed in this paper and will be referred to as TEMPO CNF.

2.3. Dispersion and film making process

The unfunctionalized, sulfonated, and TEMPO CNF were dispersed in DMF and water to make 0.1 wt% solids suspensions (30 g total weight). These were then homogenized with an IKA T18 basic Ultra-Turrax for 5 min (at a setting of 1) followed by another 5 min (at a setting of 2) before being sonicated in a bath sonicator (Branson 3510R-MT, 100 W, 42 kHz) for 3 days in a 50 mL polypropylene centrifuge tube. The samples' transparency was measured with ultraviolet-visible

Table 1
Summary of characteristics of the unfunctionalized and functionalized CNF.

Samples	Sulfur Content (wt%)	Degree of Substitution	mmol of sulfate groups/ g of cellulose	CI (%)[a]	Zeta Potential (mV)	Transmittance at 600 nm (%)[b]	Transmittance at 600 nm (%)[c]
unfunctionalized CNF	0	0	0	75	−25 ± 2	2	31
TEMPO CNF	0	0.30	0	77	−49 ± 4	17	73
SCNF1-5	1.7	0.09	0.56	73	−39 ± 1	9	60
SCNF1-30	2.3	0.12	0.74	72	−43 ± 2	12	76
SCNF1-60	2.6	0.14	0.86	72	−43 ± 2	13	80
SCNF2-5	2.5	0.14	0.86	69	−45 ± 2	9	67
SCNF2-30	3.9	0.22	1.36	65	−47 ± 2	28	75
SCNF2-60	4.5	0.26	1.60	59	−43 ± 2	29	82
SCNF3-5	3.7	0.21	1.30	70	−40 ± 2	12	69
SCNF3-30	4.3	0.24	1.48	57	−44 ± 1	34	78
SCNF3-60	5.0	0.29	1.79	53	−48 ± 1	36	82

[a] Crystallinity index.
[b] CNF dispersed in DI water (0.1 wt%).
[c] CNF dispersed in DMF (0.1 wt%).

spectroscopy (UV-vis) to assess dispersion. The DMF/CNF and water/CNF dispersion were cast in a glass petri dish and put in an oven at 30 °C with airflow to make films. The films were used for wide angle x-ray diffraction (WAXD) and Fourier transform infrared spectroscopy (FTIR).

2.4. Characterization

A total of eleven different CNF sample types were investigated and characterized in this study, as summarized in Table 1. Scanning electron microcopy (SEM) was completed using a Zeiss Ultra60 FE-SEM, in which samples were dispersed at 0.02 wt% in DMF (approach similar to that outlined above) and then drop casted on a conductive substrate (samples we not coated prior to imaging). Elemental analysis was performed by Atlantic Microlab Inc. to measure the sulfur content. The CNF were freeze dried followed by vacuum drying before testing. The testing was done using a Carlo Erba 1108 Elemental Analyzer. The samples were weighed, combusted, separated by gas chromatography, and then the sulfur amount was measured by thermal conductivity. The degree of substitution for the sulfonated samples were calculated based on the sulfur content and the equation used can be found in the Supplementary information. The degree of substitution for the TEMPO CNF was determined with conductometric titration and the procedure can be found in the Supplementary information (Habibi et al., 2006).

WAXD was used to assess crystallinity index (CI) changes between the neat and functionalized CNF. Measurements were completed on a Rigaku MicroMax-002 (CuK_α, $\lambda = 0.1542$ nm) equipped with a Rigaku R-axis IV++ detector, and the data was analyzed with MDI Jade 9 software. The CI of the samples were determined by the peak height method (Segal method) (Park, Baker, Himmel, Parilla, & Johnson, 2010; Segal, Creely, Martin, & Conrad, 1959), and is calculated with Eq. (1), with I_{002} being the peak height at $2\theta = \sim 23^\circ$, and I_{am} being the minimum value at $2\theta = \sim 18.5^\circ$.

$$Crystallinity\ Index\ (\%) = \left(\frac{I_{002} - I_{am}}{I_{002}}\right) \times 100 \quad (1)$$

FTIR was completed on a Spectrum One (PerkinElmer, Inc.) to observe if there were any differences between the unfunctionlized, sulfonated, and TEMPO CNF. FTIR was done in transmission mode with pellets of KBr and the cast films. To make the pellets for FTIR, KBr and the cast films were ground into a powder and then pressed into a pellet using a KBr pellet die from International Crystal Laboratories. The scan range was 750 cm^{-1} to 2000 cm^{-1} with a resolution of 4 cm^{-1} with 128 scans. Zeta potential was completed on a ZEN 3690 (Malvern Instruments) with 0.005 wt% samples in 0.5 mM NaCl aqueous solutions. UV–vis was used to determine the quality of dispersion of the CNF. The measurements were completed on a Lambda 35 (PerkinElmer Co.) with quartz cuvettes with a scan speed of 480 nm/min with a resolution of 1 nm over a range of 400–700 nm.

3. Results and discussion

3.1. Change in morphology

The morphology of the unfunctionalized CNF, TEMPO CNF, and SCNF3-60 are shown in Fig. 1, and SEM images of all samples can be found in Fig. S1. Unfunctionalized CNF have a fibril-like morphology with high aspect ratio, and form a dense network structure. The TEMPO CNF also has a fibril-like morphology with a lower aspect ratio, and was well dispersed on the imaging substrate. For the sulfonated CNF, all reaction times at all CSA to AGU reaction ratios show differences in the overall particle morphology (e.g. shorter, thinner diameter, less bundled) and network formation, but in general still retain a fibril-like morphology. In contrast, previous works on sulfonation of cellulosic material were usually done to make highly soluble cellulose sulfate that did not retain their morphology (Schweiger, 1972; Svensson et al., 2005; Zhang et al., 2011). Though there have been some studies that show sulfonated cellulosic materials retaining a fiber morphology, these cases used large starting diameter materials like cotton pulp with short reaction times, and the functionalized fibers typically have large diameters (> 20 μm) (Nourani et al., 2016). In contrast, by using CNF as a starting material our sulfonated CNF had diameters less than 100 nm, and retained their fibril-like morphology with no observable agglomeration.

3.2. Elemental analysis and FTIR

Elemental analysis confirmed there was no sulfur in the unfunctionalized CNF and TEMPO CNF, which was expected (Table 1). With increasing reaction time the sulfur content increases in the sulfonated samples at the same CSA to AGU ratio. Also with higher CSA to AGU ratio the sulfur content was higher at the same reaction time. The SCNF2-60 sample had 4.5 wt% sulfur and the SCNF3-60 had 5 wt%, suggesting a leveling off of functionalization while maintaining the CNF fibril-like morphology. The theoretical maximum amount of sulfur if all hydroxyls were functionalized would result in ~24 wt% sulfur. The sulfonation reaction was relatively initially quick; where for the three different CSA to AGU reactions over 50% of the sulfur content was on the CNF after 5 min of reaction time, as compared to after 60 min of reaction time.

The FTIR spectra (Figs. 2 and S2) were normalized to the peak at 1112 cm^{-1} (stretching of the C−O−C and in-phase ring wagging), because the functionalization should have little effect on it (Klemm, Philipp, Heinze, Heinze, & Wagenknecht, 1998a). The peak around

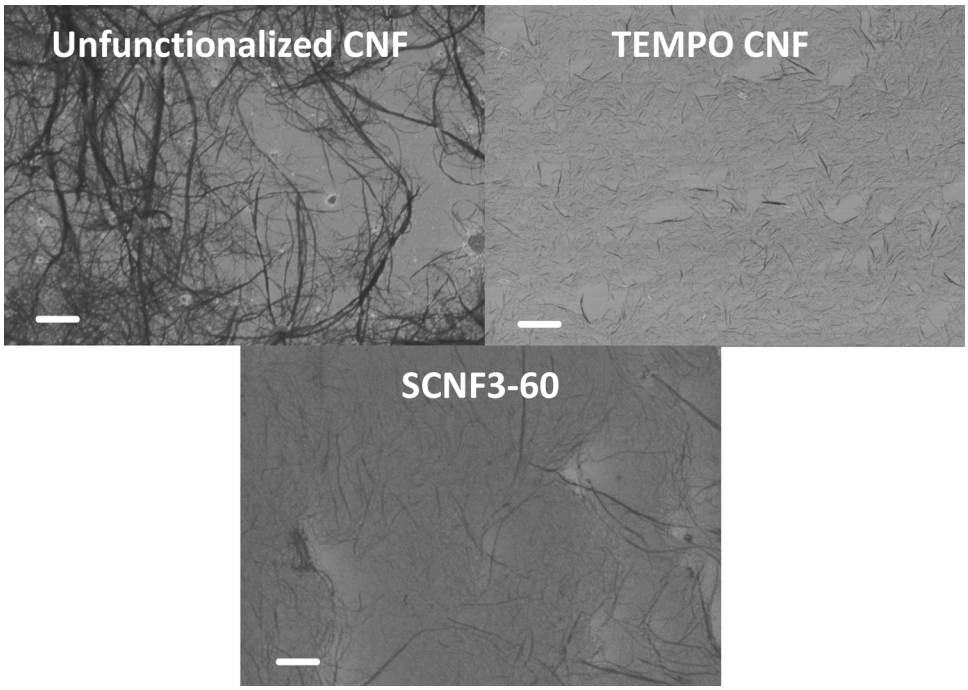

Fig. 1. SEM images of the unfunctionalized CNF, TEMPO CNF, and SCNF3-60 showing that SCNF3-60 still retain fibril-like morphology. The TEMPO CNF seems to display a shorter morphology than the unfunctionalized and SCNF3-60. Scale bar is 2 μm.

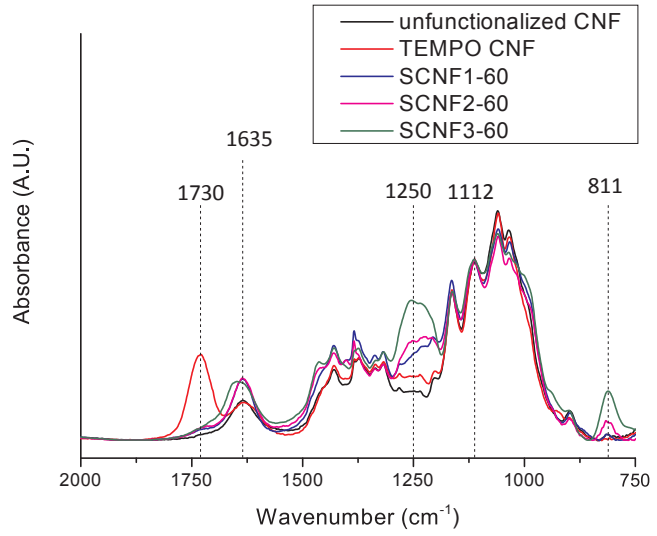

Fig. 2. FTIR spectra of the CNF films (cast from CNF-water suspension) showing differences in peaks between unfunctionalized and functionalization CNF.

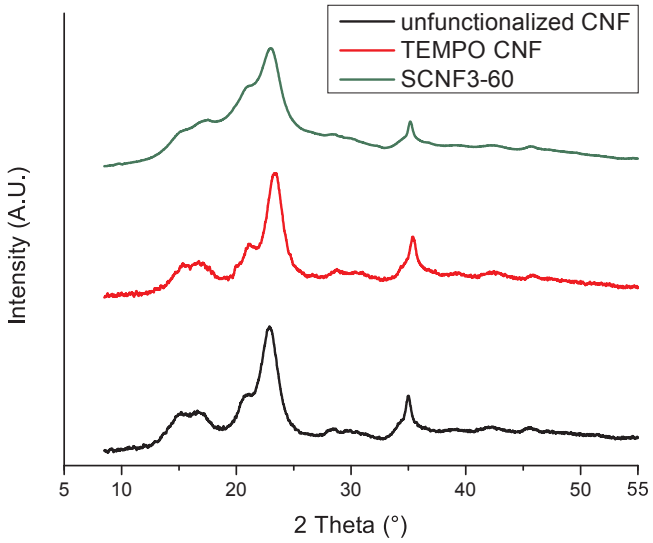

Fig. 3. WAXD integral scan of the unfunctionalized TEMPO CNF, and SCNF3-60.

1635 cm^{-1} is typically associated with bound water, while the SCNF3-60 displayed a bound water peak at 1647 cm^{-1}. The 1730 cm^{-1} peak is associated with the acid form of carboxyl groups (COOH) (Fujisawa, Okita, Fukuzumi, Saito, & Isogai, 2011; Saito, Nishiyama, Putaux, Vignon, & Isogai, 2006). The sulfonated CNF have 2 new peaks, a broad peak at 1250 cm^{-1} and a relatively narrow peak at 811 cm^{-1} associated with S═O and C—O—S bonds, respectively (Gu, Catchmark, Kaiser, & Archibald, 2013). The presence of these peaks, which were not present in the unfunctionalized and TEMPO CNF, indicates that the CNFs were sulfonated. With increasing CSA to AGU ratios the 1250 and 811 cm^{-1} peaks had higher absorbance indicating the samples were more sulfonated, which is supported by the elemental analysis (Table 1). This result is expected and is consistent with literature (Lin & Dufresne, 2014b; Wang, Li, Xiao, & Wu, 2009). The exception was SCNF1-30, despite elemental analysis showing higher sulfur content than SCNF1-5, there was less absorbance than SCNF1-5, and the reason for this discrepancy is unclear.

3.3. Change in crystallinity

The 2-D WAXD patterns of unfunctionalized CNF, TEMPO CNF, and SCNF3-60 is given in Fig. 3, showing this sulfonation method can affect the crystallinity of the resulting CNF (Table 1). In general, there was a lower CI with longer reaction times and with higher CSA to AGU ratio. For comparison, the decrease in CI was much lower with the sulfonation approach used in this study than the regioselective oxidative bisulfute method (Liimatainen et al., 2013). Liimatainen et al. reported a sulfonated CNF with 0.51 mmol of sulfonated groups/g cellulose resulted in a ~54% decrease in CI (i.e. from ~65% down to ~30%). By comparison, for the SCNF1-60 sample, having similar concentration of sulfonated groups (0.56 mmol/g cellulose), had only a ~3% decrease in CI (i.e. from 75% down to 73%). Even the most sulfonated sample in our study, SCNF3-60 (1.79 mmol/g cellulose), had only a ~29% decrease in CI (i.e. from 75% down to 53%). This shows the reaction method used in this study maintains the cellulose crystal structure

much better than the regioselective oxidative bisulfite method. The retention of CI should result in higher mechanical properties of the functionalized CNF, which can be translated into higher properties of CNF films and composites.

3.4. Zeta potential

Zeta potential is the measure of the difference between the electrostatic potential of two surfaces, and can be used to assess the stability of CNF suspensions (Hunter, 1988; Okita, Fujisawa, Saito, & Isogai, 2010). The zeta potential of each sample in 0.5 mM NaCl aqueous solution, was −25 mV, −49 mV and −39 to −48 mV for unfunctionalized, TEMPO, and sulfonated CNFs, respectively. This zeta potential measured for unfunctionalized CNF is consistent with what is reported in other studies for cellulose (Reischl, Stana-Kleinschek, & Ribitsch, 2006; Tonoli et al., 2012). For the sulfonated samples, in general, for the same CSA to AGU ratio longer reaction times typically lead to slightly higher zeta potentials. The highest zeta potential was −48 mV for SCNF3-60, which had the longest reaction time at the highest CSA to AGU ratio. Interestingly, when extending sulfonation reaction times beyond the initial 5 min reaction (i.e. SCNF1-5, SCNF2-5, and SCNF3-5), the change in zeta potential with increasing sulfur content was minimal, suggesting that the surface of the fibrils reacts quickly and reach a saturated state. Further sulfonation seems to only marginally increase the zeta potential. This may be due to additional sulfur groups being located below the fibril surface where they are shielded from solution and are not able to contribute to the surface charge. This is somewhat corroborated by the decrease in crystallinity with increasing sulfur content, suggesting that the cellulose chains become less ordered with increased sulfonation.

3.5. Dispersibility

UV–vis spectra can be used to assess the dispersion quality of suspensions, because transmittance is related to the width of the nanofiber, which in turn can be related to aggregation of the CNF (Carr & Hermans, 1978; Hantgan & Hermans, 1979; Isogai, Saito, & Fukuzumi, 2011). The UV–vis data for unfunctionalized, TEMPO, and sulfonated CNFs dispersed at 0.1 wt% either in water or in DMF is given in Figs. 4 and S3 and the transmittance values of all the samples at 600 nm are listed in Table 1. All sulfonated CNF dispersions have better transparency than the unfunctionalized CNF, and in many cases were even better than TEMPO CNF dispersion. In general, longer sulfonation times leads to higher transmittance, and there is a large increase in transparency for the sulfonated CNF between 5 and 30 min of reaction time, while there is little change in transparency between 30 and 60 min. Though the mechanism is for this behavior is unclear, it is plausible that the increase in transmittance from the unfunctionalized CNF to the 5 min sulfonated CNFs (i.e. SCNF1-5, SCNF2-5, and SCNF3-5) is a result of improved dispersion as from increased surface charge. Whereas the increase in transmittance between 5 and 30 and 60 min, is a consequence of a finer CNF morphology resulting from the sub-surface sulfonation of the CNF (see Fig. S1), allowing for increased CNF fibrillation during the homogenization steps when making dispersions used for UV–vis testing.

Our sulfonated CNF displayed significantly better transmittance in solvent compared to unfunctionalized CNF with as low as 5 min of reaction time, while the previously reported sulfonation method (regioselective oxidative bisulfute) for CNF took over 3 days of reaction time (Liimatainen et al., 2013; Sirviö et al., 2014; Sirviö, Liimatainen, Niinimäki, & Hormi, 2013). Depending on the CSA to AGU content only 30–60 min of reaction time is needed to make a sulfonated CNF that has comparable to or better transmittance in solvent than TEMPO CNF, which is shorter than the preparation time for post TEMPO treatment of existing CNFs as what was done in this study.

3.6. Effects of dispersing and/or heating in different solvents

The effects of dispersing CNF in DMF versus water, and heating of CNF-solvent suspensions on the functional groups were also studied, because materials often undergo heating in solvent in the process of making composites. Films were made by the process previously described with the 3 days of dispersion. After the dispersion half of the suspension was cast to produce films, while the other half of the suspension was then subjected to 70 °C for 3 days before being cast.

FTIR comparison of the unfunctionalized CNF films cast from CNF-DMF versus CNF-water suspensions shows there was minimal differences (Fig. 5). The SCNF3-60 sample dispersed in DMF showed a slight decrease in magnitude of the peaks associated with sulfate ester groups (1250 and 811 cm^{-1}). Additionally, there was the development of a shoulder at 1710 cm^{-1}, which could be associated with C=O in formate, and will be discussed later. The TEMPO CNF cast from DMF exhibited a broadening of and decreased amplitude of the peak associated with COOH (~1730 cm^{-1}), and also a peak develops at 1613 cm^{-1} that is associated with COO^- (Fujisawa et al., 2011; Saito et al., 2006). The decrease in the 1730 cm^{-1} peak and the newly developed 1613 cm^{-1} peak is due to the acid form carboxyl groups forming carboxyl dimethylammonium groups, and will be discussed later. The broadening of the 1730 cm^{-1} peak occurs due to the larger peaks at 1613 and 1635 cm^{-1} overlapping with the 1730 cm^{-1} peak.

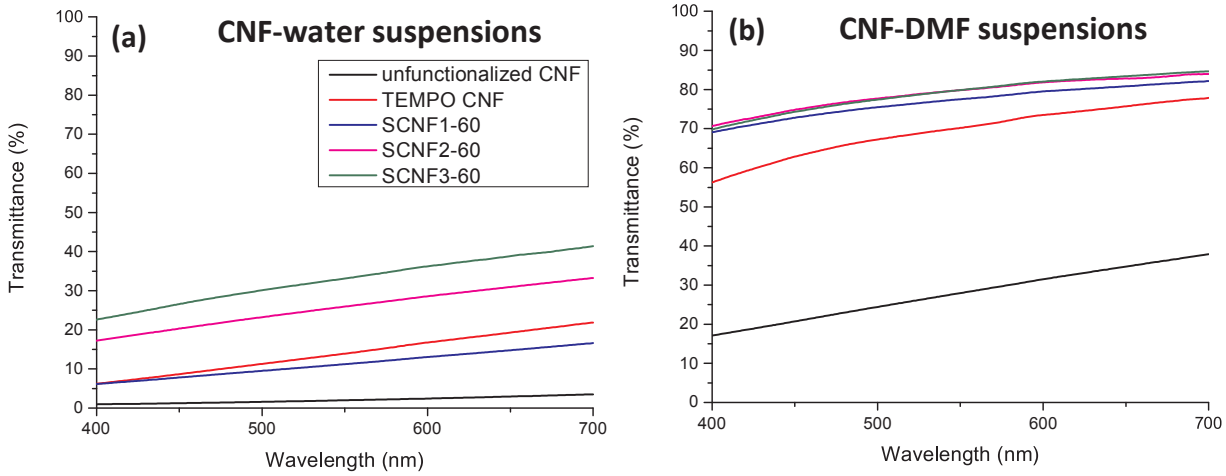

Fig. 4. UV–vis spectra of CNF dispersions in (a) water and (b) DMF after 3 days of sonication showing all functionalized samples have higher transparency than the unfunctionalized sample.

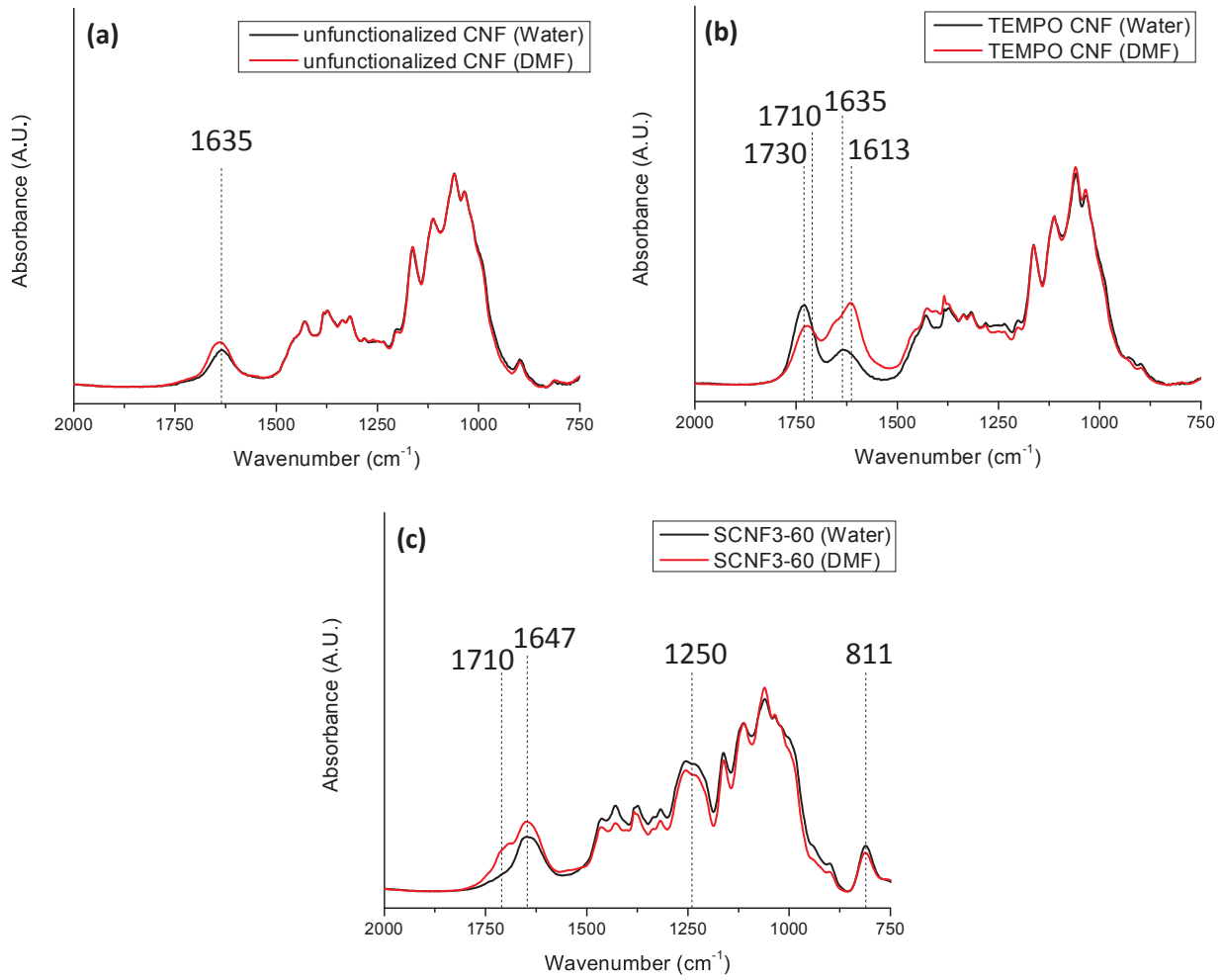

Fig. 5. Comparison of FTIR spectra of CNF film cast after being dispersed in water versus DMF (no heating). (a) unfunctionalized CNF showing no difference, (b) TEMPO CNF showing a decrease in the 1730 cm^{-1} peak and a newly developed peak at 1613 cm^{-1} associated with the COO^- when dispersed in DMF, and (c) SCNF3-60 developing shouldering at 1710 cm^{-1} when dispersed in DMF.

FTIR comparison of the films cast from CNF-water suspensions with and without heating indicates there is no change in unfunctionalized and TEMPO CNF when it was heated (Fig. 6). For SCNF3-60, there was a drastic decrease in the peak heights associated with sulfonation (1250 and 811 cm^{-1}), suggesting a cleavage of the sulfate groups off the CNF, as has been previously reported for cellulose nanocrystals when heated (Beck & Bouchard, 2014; Dong & Gray, 1997; Lewis, Derakhshandeh, Hatzikiriakos, Hamad, & MacLachlan, 2016).

FTIR comparison of the films cast from CNF-DMF suspensions with and without heating indicates there was no change in unfunctionalized and TEMPO CNF as a result of heating (Fig. 7). For the SCNF3-60 sample, a peak develops at 1710 cm^{-1}, where only a shoulder was present without heating. There was a decrease in the peaks associated with sulfonation (1250 and 811 cm^{-1}), similarly to what happened after heating the CNF-water suspensions. There was also a shoulder previously because of the larger peak at 1635 cm^{-1} for bound water before heating due to more sulfate groups and its hydrophilicity.

The mechanism for additional functionalizations to TEMPO and sulfonated CNF when dispersed in DMF occurs because dimethylformamide decomposes into formic acid and dimethylamine in the presences of water. These two compounds can undergo partial ionization to form dimethylamonnium cations and formate anions (Juillard, 1977). The decomposition of DMF can be seen in the equations below.

$$HCON(CH_3)_2 + H_2O \rightarrow HCOOH + (CH_3)_2NH \quad (2)$$

$$HCOOH + (CH_3)_2NH \leftrightarrow HCOO^- + (CH_3)_2NH_2^+ \quad (3)$$

Upon addition of CNF to DMF trace amount of water is introduced that promotes the formation of the DMF degradation products. The peak observed at 1710 cm^{-1} in the FTIR spectrum of the sulfonated samples when dispersed in DMF is typically associated with carbonyl groups, suggests that an exchange of functional groups may be occurring during mixing CNF in DMF. It is known that cellulose formate can form when formic acid is added to a cellulose/DMF suspension. The formic acid formation due to the degradation of DMF results in formate groups forming on the CNF. It has also been shown that sulfuric acid can act as a catalyst for the formation of cellulose formate (Heinze & Liebert, 2001; Klemm, Philipp, Heinze, Heinze, & Wagenknecht, 1998b). Since the sulfate groups can cleave off the cellulose into the solvent, it could help promote cellulose formate formation. This would explain why such a strong peak was seen in SCNF3-60, but not seen in the unfunctionalized and TEMPO CNF. The formation of cellulose formate can be seen in Eq. (4).

$$CNF^{SO_3^-} + [HCOOH] + [H^+] \leftrightarrow CNF^{COOH} + [SO_4]^- + [H^+] \quad (4)$$

The dimethylammonium cations can therefore undergo a neutralization reaction with the carboxylic acid groups (COO^-) of TEMPO CNF or the sulfate ester groups (SO_3^-) of the sulfonated CNF to form a dimethylammonium salt (Juillard, 1977). The reaction for TEMPO CNF after dissociating in the solvent to form carboxyl dimethylammonium can be seen below. The same reaction can possibly happen for

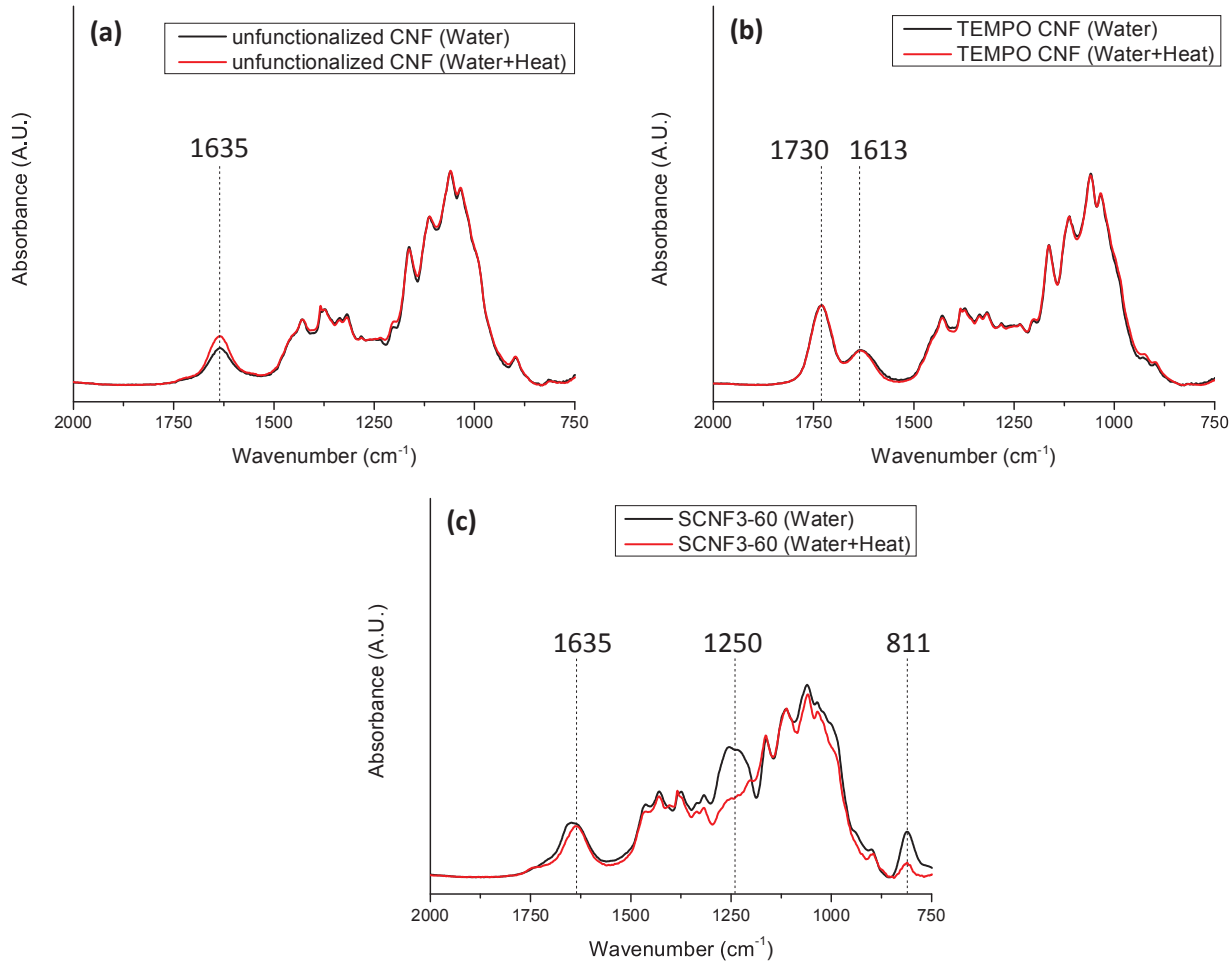

Fig. 6. Comparison of FTIR spectra of CNF dispersed in water (no heating) and cast versus the dispersion heated for 3 days at 70 °C then cast. After heating the (a) unfunctionalized CNF shows no change, (b) TEMPO CNF shows no change, and (c) SCNF3-60 shows a decrease in the 1250 and 811 cm^{-1} due to cleavage of the sulfate groups.

sulfonated CNF in the equations below the COO^- can be replaced with SO_3^- representing the sulfate group after dissociating.

$$_{CNF}COO^- + (CH_3)_2NH_2^+ \leftrightarrow [_{CNF}COO^-][(CH_3)_2NH_2^+] \quad (5)$$

Evidence for this type of reaction can be seen by examining the FTIR spectrum of the TEMPO CNF (Fig. 5) that shows a decrease in the peak associated with COOH and a newly developed peak associated with COO^- when dispersed in DMF. This peak associated with COO^- was not seen when the TEMPO CNF was dispersed in water. This peak at 1613 cm^{-1} associated with COO^- does not exist in the sulfonated and unfunctionalized CNF films whether they were cast from water or DMF.

To further support the formation of this dimethylammonium functional group on the CNF, when TEMPO and sulfonated CNF–DMF suspensions were heated at 70 °C for 3 days, the suspensions turned yellowish with TEMPO CNF being more yellow than the sulfonated CNF (Fig. S4). This yellowing was not seen in the unfunctionalized CNF heated in DMF, and any of the CNF samples when heated in water. Previously it was shown that CNF film functionalized with an ammonium carboxylate group ($COONH_4$) would turn yellow after undergoing heating, though the reason for yellowing was unclear (Shimizu, Fukuzumi, Saito, & Isogai, 2013). The dimethylammonium carboxyl CNF derivative is similar in chemistry to the CNF functionalized with an ammomnium carboxylate group mentioned above and should behave similarly. The amount of yellowing is possibly an indicator of how much dimethylammonium has neutralized the ionized groups on the CNF, which would mean it is more prominent in the TEMPO CNF than the sulfonated CNF.

To test the possibility that the yellowing of TEMPO CNF in DMF was a result of inadequate removal of reagents used for the functionalization, separate dispersions of TEMPO, NaCl, and HClO in DMF were left at 70 °C for 3 days. It was found that none of these chemicals in DMF or DMF itself turned yellow. Fig. S5 contains images of these results. Acetic acid, which has a similar functional group to the TEMPO CNF (carboxylic acid), was also mixed with DMF and heated as previously described and it also did not lead to a yellowing of the solution (Fig. S5).

4. Conclusion

Existing CNF were successfully sulfonated with a DMF and CSA solution resulting in a sulfonated CNF with a high surface charge while retaining a fibril-like morphology. This one step reaction is relatively rapid, and a reaction time of as little as 5 min leads to a significant increase in the zeta potential and dispersibility in water and DMF when compared to unfunctionalized CNF. A post-TEMPO oxidation treatment on existing CNF and regioselective bisulfite oxidation method can yield CNF with similar dispersibility but they require multiple step reactions and longer reaction times. For sulfonated CNF, higher CSA to AGU ratio, and longer reaction times leads to higher sulfur content on the CNF and also lower crystallinity. This decrease in crystallinity was much less than the regioselective bisulfite process reported in the literature for the same amount of sulfonation. It was observed that when TEMPO and sulfonated CNF were dispersed in DMF additional functionalization occurred that did not happen with unfunctionalized CNF. The TEMPO CNF's additional functionalization seems to be mainly dimethylammonium carboxyl groups, and the sulfonated CNF's

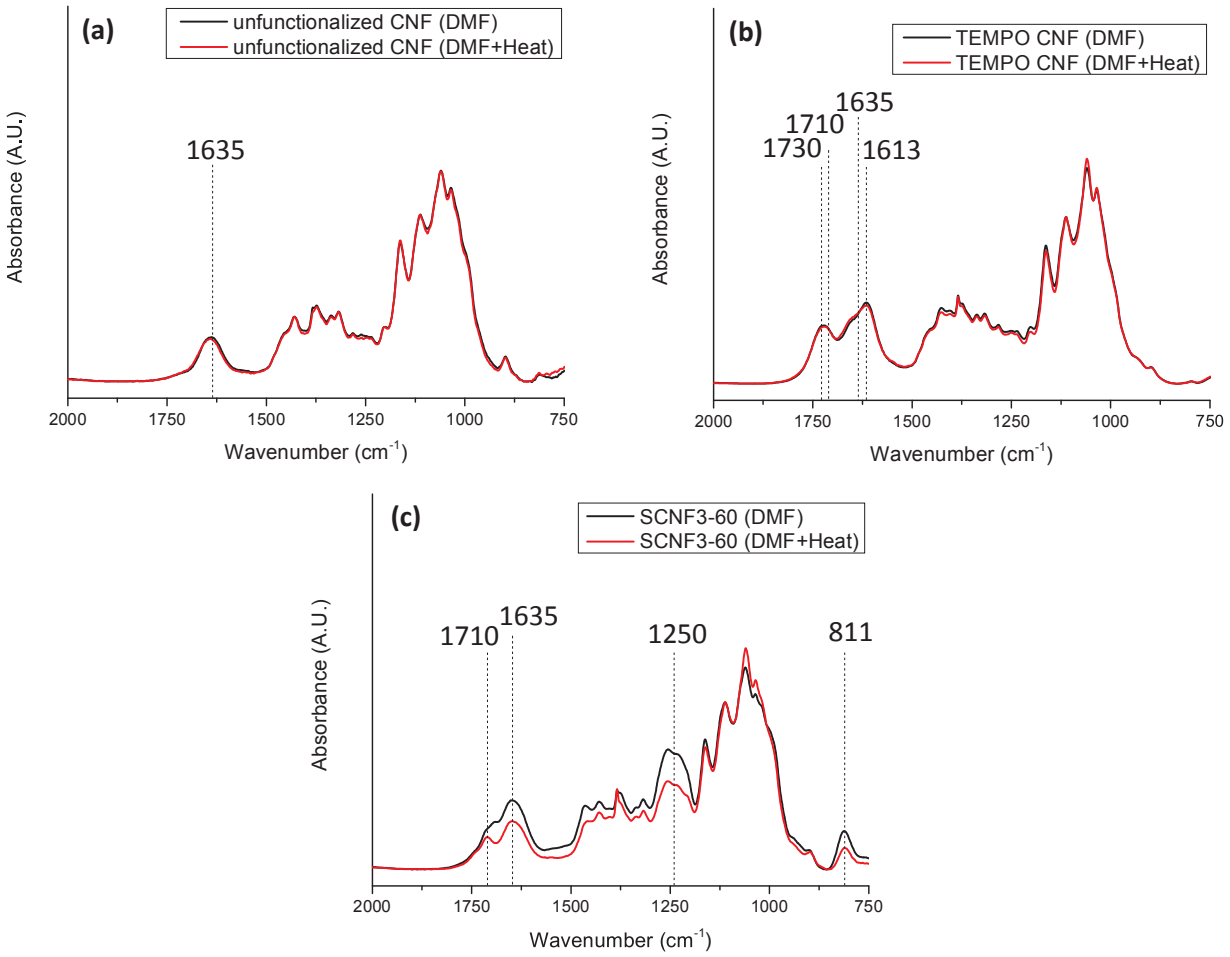

Fig. 7. Comparison of FTIR spectra of CNF dispersed in DMF (no heating) and versus the dispersion heated for 3 days at 70 °C then cast. After heating the (a) unfunctionalized CNF shows no difference, (b) TEMPO CNF shows no difference, and (c) SCNF3-60 showing a decrease in the 1250 and 811 cm^{-1} due to cleavage of the sulfate groups. Also a decrease in the 1635 cm^{-1} peak and the shoulder at 1710 cm^{-1} developing into a peak.

additional functionalization seems to be mainly cellulose formate. These results suggest that this post sulfonation method can be used to rapidly tailor the dispersibility of unfunctionalized CNF for a wide range of applications.

Acknowledgments

This work was financially supported by the Renewable Bioproducts Institute at Georgia Institute of Technology, the Air Force Office of Scientific Research (Grant# FA9550-14-1-0194), and by the Forest Products Laboratory (USDA grant # 15-JV-11111129-063).

Appendix A. Supplementary data

Supplementary data associated with this article can be found, in the online version, at http://dx.doi.org/10.1016/j.carbpol.2017.10.077.

References

Araki, J., Wada, M., & Kuga, S. (2001). Steric stabilization of a cellulose microcrystal suspension by poly(ethylene glycol) grafting. *Langmuir, 17*(1), 21–27.
Beck, S., & Bouchard, J. (2014). Auto-catalyzed acidic desulfation of cellulose nanocrystals. *Nordic Pulp & Paper Research Journal, 29*(1), 6–14.
Carr, M. E., Jr., & Hermans, J. (1978). Size and density of fibrin fibers from turbidity. *Macromolecules, 11*(1), 46–50.
Chang, H., Chien, A.-T., Liu, H. C., Wang, P.-H., Newcomb, B. A., & Kumar, S. (2015). Gel spinning of polyacrylonitrile/cellulose nanocrystal composite fibers. *ACS Biomaterials Science & Engineering, 1*(7), 610–616.
Chang, H., Luo, J., Bakhtiary Davijani, A. A., Chien, A.-T., Wang, P.-H., Liu, H. C., et al. (2016). Individually dispersed wood-based cellulose nanocrystals. *ACS Applied Materials & Interfaces, 8*(9), 5768–5771.
Chang, H., Luo, J., Gulgunje, P. V., & Kumar, S. (2017). Structural and functional fibers. *Annual Review of Materials Research, 47*, 331–359.
Chen, W., Lickfield, G. C., & Yang, C. Q. (2004). Molecular modeling of cellulose in amorphous state. Part I: Model building and plastic deformation study. *Polymer, 45*(3), 1063–1071.
Dong, X. M., & Gray, D. G. (1997). Effect of counterions on ordered phase formation in suspensions of charged rodlike cellulose crystallites. *Langmuir, 13*(8), 2404–2409.
Espino-Pérez, E., Domenek, S., Belgacem, N., Sillard, C. C., & Bras, J. (2014). Green process for chemical functionalization of nanocellulose with carboxylic acids. *Biomacromolecules, 15*(12), 4551–4560.
Fujisawa, S., Okita, Y., Fukuzumi, H., Saito, T., & Isogai, A. (2011). Preparation and characterization of TEMPO-oxidized cellulose nanofibril films with free carboxyl groups. *Carbohydrate Polymers, 84*(1), 579–583.
Gu, J., Catchmark, J. M., Kaiser, E. Q., & Archibald, D. D. (2013). Quantification of cellulose nanowhiskers sulfate esterification levels. *Carbohydrate Polymers, 92*(2), 1809–1816.
Habibi, Y., Chanzy, H., & Vignon, M. R. (2006). TEMPO-mediated surface oxidation of cellulose whiskers. *Cellulose, 13*(6), 679–687.
Habibi, Y., Lucia, L. A., & Rojas, O. J. (2010). Cellulose nanocrystals: Chemistry, self-assembly, and applications. *Chemical Reviews, 110*(6), 3479–3500.
Habibi, Y. (2014). Key advances in the chemical modification of nanocelluloses. *Chemical Society Reviews, 43*(5), 1519–1542.
Hantgan, R. R., & Hermans, J. (1979). Assembly of fibrin. A light scattering study. *Journal of Biological Chemistry, 254*(22), 11272–11281.
Heinze, T., & Liebert, T. (2001). Unconventional methods in cellulose functionalization. *Progress in Polymer Science, 26*(9), 1689–1762.
Hunter, R. J. (1988). *Zeta potential in colloid science: Principles and applications.* San Diego: Academic Press.
Isogai, A., Saito, T., & Fukuzumi, H. (2011). TEMPO-oxidized cellulose nanofibers. *Nanoscale, 3*(1), 71–85.
Isogai, A. (2013). Wood nanocelluloses: Fundamentals and applications as new bio-based nanomaterials. *Journal of Wood Science, 59*(6), 449–459.
Juillard, J. (1977). Dimethylformamide: Purification, tests for purity and physical properties. *Pure and Applied Chemistry, 49*(16), 885–892.

Klemm, D., Philipp, B., Heinze, T., Heinze, U., & Wagenknecht, W. (1998a). *Comprehensive cellulose chemistry volume 1: Fundamentals and analytical methods.* Weinheim: Wiley-VCH.

Klemm, D., Philipp, B., Heinze, T., Heinze, U., & Wagenknecht, W. (1998b). *Comprehensive cellulose chemistry volume 2: Funtionalization of cellulose.* Weinheim: Wiley-VCH.

Lewis, L., Derakhshandeh, M., Hatzikiriakos, S. G., Hamad, W. Y., & MacLachlan, M. J. (2016). Hydrothermal gelation of aqueous cellulose nanocrystal suspensions. *Biomacromolecules, 17*(8), 2747–2754.

Liimatainen, H., Visanko, M., Sirviö, J., Hormi, O., & Niinimäki, J. (2013). Sulfonated cellulose nanofibrils obtained from wood pulp through regioselective oxidative bisulfite pre-treatment. *Cellulose, 20*(2), 741–749.

Lin, N., & Dufresne, A. (2014a). Nanocellulose in biomedicine: Current status and future prospect. *European Polymer Journal, 59*, 302–325.

Lin, N., & Dufresne, A. (2014b). Surface chemistry, morphological analysis and properties of cellulose nanocrystals with gradiented sulfation degrees. *Nanoscale, 6*(10), 5384–5393.

Luo, J., Chang, H., Davijani, A. A. B., Liu, H. C., Wang, P.-H., Moon, R. J., et al. (2017). Influence of high loading of cellulose nanocrystals in polyacrylonitrile composite films. *Cellulose,* 1–14.

Moon, R. J., Schueneman, G. T., & Simonsen, J. (2016). Overview of cellulose nanomaterials, their capabilities and applications. *The Journal of The Minerals, Metals & Materials Society, 68*(9), 2383–2394.

Nagasawa, K., Tohira, Y., Inoue, Y., & Tanoura, N. (1971). Reaction between carbohydrates and sulfuric acid: Part I. Depolymerization and sulfation of polysaccharides by sulfuric acid. *Carbohydrate Research, 18*(1), 95–102.

Nechyporchuk, O., Belgacem, M. N., & Bras, J. (2016). Production of cellulose nanofibrils: A review of recent advances. *Industrial Crops and Products, 93*, 2–25.

Nourani, M., Baghdadi, M., Javan, M., & Bidhendi, G. N. (2016). Production of a biodegradable flocculant from cotton and evaluation of its performance in coagulation-flocculation of kaolin clay suspension: Optimization through response surface methodology (RSM). *Journal of Environmental Chemical Engineering, 4*(2), 1996–2003.

Okita, Y., Fujisawa, S., Saito, T., & Isogai, A. (2010). TEMPO-oxidized cellulose nanofibrils dispersed in organic solvents. *Biomacromolecules, 12*(2), 518–522.

Park, S., Baker, J. O., Himmel, M. E., Parilla, P. A., & Johnson, D. K. (2010). Cellulose crystallinity index: Measurement techniques and their impact on interpreting cellulase performance. *Biotechnology for Biofuels, 3*(1), 10.

Reischl, M., Stana-Kleinschek, K., & Ribitsch, V. (2006). Electrokinetic investigations of oriented cellulose polymers. *Macromolecular Symposia, 244*, 31–47 (Wiley Online Library).

Saito, T., Nishiyama, Y., Putaux, J.-L., Vignon, M., & Isogai, A. (2006). Homogeneous suspensions of individualized microfibrils from TEMPO-catalyzed oxidation of native cellulose. *Biomacromolecules, 7*(6), 1687–1691.

Saito, T., Kimura, S., Nishiyama, Y., & Isogai, A. (2007). Cellulose nanofibers prepared by TEMPO-mediated oxidation of native cellulose. *Biomacromolecules, 8*(8), 2485–2491.

Schweiger, R. G. (1972). Polysaccharide sulfates. I. Cellulose sulfate with a high degree of substitution. *Carbohydrate Research, 21*(2), 219–228.

Schweiger, R. G. (1979). New cellulose sulfate derivatives and applications. *Carbohydrate Research, 70*(2), 185–198.

Segal, L., Creely, J., Martin, A., Jr., & Conrad, C. (1959). An empirical method for estimating the degree of crystallinity of native cellulose using the X-ray diffractometer. *Textile Research Journal, 29*(10), 786–794.

Shimizu, M., Fukuzumi, H., Saito, T., & Isogai, A. (2013). Preparation and characterization of TEMPO-oxidized cellulose nanofibrils with ammonium carboxylate groups. *International Journal of Biological Macromolecules, 59*, 99–104.

Siqueira, G., Bras, J., & Dufresne, A. (2010). Cellulosic bionanocomposites: A review of preparation, properties and applications. *Polymers, 2*(4), 728–765.

Siró, I., & Plackett, D. (2010). Microfibrillated cellulose and new nanocomposite materials: A review. *Cellulose, 17*(3), 459–494.

Sirviö, J. A., Liimatainen, H., Niinimäki, J., & Hormi, O. (2013). Sustainable packaging materials based on wood cellulose. *RSC Advances, 3*(37), 16590–16596.

Sirviö, J. A., Kolehmainen, A., Visanko, M., Liimatainen, H., Niinimäki, J., & Hormi, O. E. (2014). Strong, self-standing oxygen barrier films from nanocelluloses modified with regioselective oxidative treatments. *ACS Applied Materials & Interfaces, 6*(16), 14384–14390.

Svensson, A., Nicklasson, E., Harrah, T., Panilaitis, B., Kaplan, D., Brittberg, M., et al. (2005). Bacterial cellulose as a potential scaffold for tissue engineering of cartilage. *Biomaterials, 26*(4), 419–431.

Tonoli, G., Teixeira, E., Corrêa, A., Marconcini, J., Caixeta, L., Pereira-da-Silva, M., et al. (2012). Cellulose micro/nanofibres from Eucalyptus kraft pulp: Preparation and properties. *Carbohydrate Polymers, 89*(1), 80–88.

Viet, D., Beck-Candanedo, S., & Gray, D. G. (2007). Dispersion of cellulose nanocrystals in polar organic solvents. *Cellulose, 14*(2), 109–113.

Wang, Z. M., Li, L., Zheng, B. S., Normakhamatov, N., & Guo, S. Y. (2007). Preparation and anticoagulation activity of sodium cellulose sulfate. *International Journal of Biological Macromolecules, 41*(4), 376–382.

Wang, Z.-M., Li, L., Xiao, K.-J., & Wu, J.-Y. (2009). Homogeneous sulfation of bagasse cellulose in an ionic liquid and anticoagulation activity. *Bioresource Technology, 100*(4), 1687–1690.

Wu, X., Moon, R. J., & Martini, A. (2014). Tensile strength of Iβ crystalline cellulose predicted by molecular dynamics simulation. *Cellulose, 21*(4), 2233–2245.

Zhang, K., Peschel, D., Bäucker, E., Groth, T., & Fischer, S. (2011). Synthesis and characterisation of cellulose sulfates regarding the degrees of substitution, degrees of polymerisation and morphology. *Carbohydrate Polymers, 83*(4), 1659–1664.